JOURNAL OF CATALYSIS **167,** 180–186 (1997)
ARTICLE NO. CA971531

Studies on Pt_xSn_y Bimetallics in NaY

II. Further Characterization and Catalytic Properties in the Dehydrogenation and Hydrogenolysis of Propane

P. Mériaudeau,[1] A. Thangaraj,[2] J. F. Dutel, and C. Naccache

Institut de Recherches sur la Catalyse, CNRS, 2 avenue A. Eintein, 69626 Villeurbanne Cédex, France

Received August 12, 1996; accepted November 20, 1996

CO adsorption and desorption, as studied by IR spectroscopy and mass spectrometry has been used to characterize PtNaY and Pt_xSn_yNaY samples. The change observed between adsorbed CO spectra and CO TPD has been attributed to an increase of the particle sizes due to the addition of Sn to Pt. The catalytic properties of these materials were studied by using propane dehydrogenation and propane hydrogenolysis. The TOF of propene formation is nearly the same for all samples and the apparent activation energy remains unchanged, indicating that no change in the Pt dehydrogenation properties is induced by adding Sn. In contrast the hydrogenolysis properties are deeply depressed by alloying Pt to Sn, these changes being attributed to a dilution effect rather than to an electronic effect.

INTRODUCTION

The use of bimetallic PtSn in reforming reaction is well documented: a considerable number of investigations aiming to describe the effect of tin addition to platinum have appeared (1–4). More recently, PtSn bimetallic either in the form of single crystal (5) or supported in KL zeolite has been investigated in order to determine the effect of the tin on the catalytic properties, in particular for dehydrogenation reactions (6).

In a recent issue of this journal, we described the preparation and the characterization of PtSn bimetallics in NaY host (7). Small particles of bimetallics have been formed in NaY by reacting $Sn(CH_3)_4$ with hydrogen chemisorbed on the Pt surface. The bimetallic particles contain the two elements Pt^0 and Sn^0 as observed by XPS. CO adsorption studies have shown that Sn atoms are diluting Pt atoms. In this paper, additional characterization results are presented, in particular TPD of CO coupled with IR studies. Propane dehydrogenation and propane hydrogenolysis have been used to characterize the catalytic properties of these materials.

EXPERIMENTAL

Preparation of the Catalysts

The preparation was fully described in (7) and we will briefly summarize the most important points.

NaY zeolite, was ion exchanged with Pt^{2+} amine aqueous solution, the Pt loading being 1.7 wt%. The Pt exchanged sample was dried and calcined under O_2 from room temperature to 593 K (ramping 0.2 K/min) and after 2 h at 593 K, O_2 was replaced by N_2, and the sample was reduced under a flow of H_2, T being increased from 593 to 773 K (0.5 K/min). After 2 h at 773 K, H_2 was flushed with N_2 and the sample cooled down to RT. The as prepared sample was utilized as starting material for preparing tin loaded samples. In a cell identical to that described in (8) a mixture of tetramethyl tin and *n*-hexane was contacted with the sample precovered with hydrogen. After the mixture was left in contact with the PtNaY sample overnight, the liquid was removed by evaporation through a vacuum line and the sample was evacuated, T being increased from RT to 473 K (ramping 0.5 K/min). After 2 h at 473 K, the sample was reduced under a flow of hydrogen, T being increased to 773 K (ramping 0.5 K/min).

After H_2 was flushed by N_2, the sample was cooled to RT and used for characterization and catalytic purposes.

CO chemisorption and desorption studies. The samples were pressed into thin wafers (15 mg, 18 mm diameter) and the disc was mounted into an IR cell described earlier (9) allowing *in situ* studies at different temperatures.

In order to ensure a proper heat transfer through the pellet, the wafer was mounted onto the sample holder together with a CaF_2 plate having the same size as the sample wafer. The temperature was controlled by a thermocouple inserted between the sample holder and the CaF_2 plate. The reproducibility of the TPD experiments is better than 5 K.

The IR cell was connected to a stainless UHV system allowing vacuum better than 1.310^{-4} Pa equipped with a Leybold Inficon Quadrex 20 mass spectrometer for gas

---

[1] To whom correspondence should be addressed.

[2] Permanent address: Engelhard Corp., Iselin, NJ.

phase analysis. IR spectra were registered on a Brucker IFS 48 FT IR spectrometer.

Experimental procedure for IR TPD experiments. After the sample wafer was mounted in the IR cell, outgassing was performed for 16 h at RT. The sample was then heated up to 573 K (3 K/min) and outgassed at this temperature for 3 h before contacting the sample with 0.66 kPa of H_2, the temperature being raised to 773 K (10 K/min). After 4 h at 773 K, the gas phase was removed and the sample was cooled to RT. 0.6 kPa of CO was added in the IR cell. After 10 min, the CO gas phase was removed. The TPD of adsorbed CO was performed, the sample being heated at 5 K/min and the mass number 28 being recorded with a sequence of 10 s; simultaneously the IR spectrum of adsorbed CO was registered with a sequence of 2 min. A blank experiment was performed following each TPD and IR experiments in order to know the response of the cell and to correct the base line. CO gas (99.99 purity) was from Air Liquide and has been purified by flowing through a molecular sieve unit.

Catalytic measurements. The dehydrogenation of propane (99.99 purity, from Air Liquide) was studied using a dynamic flow microreactor at atmospheric pressure. The catalyst weight and the flow of reactant were adjusted in order to have no kinetic limitation due to the thermodynamic equilibrium or to external diffusion. Reactant and products were analyzed by gas chromatography, the chromatograph being equipped with a Unibeds column (Altech, France).

RESULTS AND DISCUSSION

TPD of CO

The TPD profiles derived from mass number 28 for CO adsorbed on $Pt_{1.7}NaY$ and $Pt_{1.7}Sn_{0.9}NaY$ are shown in Fig. 1.

This figure indicates that the number of adsorbed CO molecules is larger for Pt sample compared to PtSn sample, the ratio being close to 1.9, in good agreement with results reported earlier (7). The TPD profile of $Pt_{1.7}NaY$ is characterized essentially by two peaks, one having a maximum close to 353 K and the other much broader ranging between 473 and 673 K. This CO TPD curve is nearly the same as that obtained earlier (10) for a higher Pt loading (5 wt%). The addition of Sn to Pt has a dramatic effect on the CO TPD curve: the CO molecules are desorbed at a much lower temperature compared to pure PtNaY sample. Thus, it appears that the Pt–CO bond strength is weakened by the addition of tin.

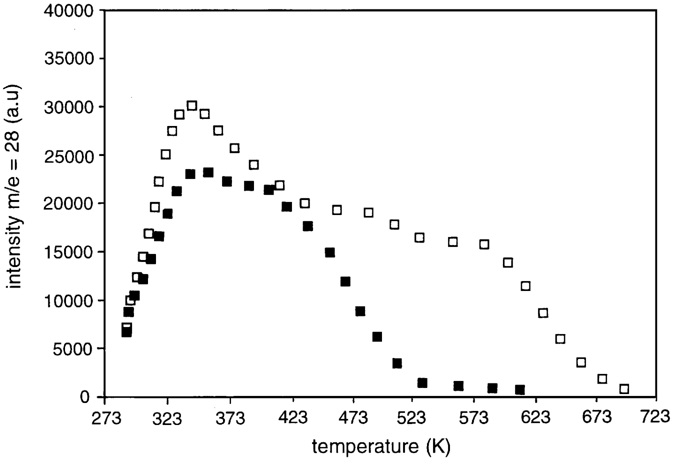

FIG. 1. TPD of CO on $Pt_{1.7}NaY$ (□) and $Pt_{1.7}Sn_{0.9}NaY$ (■) samples. Temperature ramping 5 K/min.

IR spectroscopy results. Figures 2 and 3 show the IR spectra of adsorbed CO on $Pt_{1.7}NaY$ and on $Pt_{1.7}Sn_{0.9}NaY$ and their change versus desorption temperature. As indicated earlier (7) the IR spectrum of pure Pt sample exhibited a strong carbon monoxide stretching frequency at ∼2080 cm^{-1} (full CO coverage) attributed to Pt–CO singleton vibrator and a weak shoulder at 2000 cm^{-1}. At lower wave numbers (1850 cm^{-1}) a weak vibration is attributed to bridged or triply bonded CO species (7). For $Pt_{1.7}Sn_{0.9}NaY$ sample the Pt–CO singleton vibrator has a wave number shifted to lower value compared to pure Pt and the bridged CO species are no more existing. These two differences between CO on $Pt_{1.7}NaY$ and on $Pt_{1.7}Sn_{0.9}NaY$ have been attributed to the presence of Sn (7) and were considered as an evidence of the dilution of Pt atoms by tin atoms.

The interesting point of the comparison between IR and TPD results is that for $T > 523$ K no CO remains adsorbed on $Pt_{1.7}Sn_{0.9}NaY$, whereas some CO molecules remain adsorbed on the $Pt_{1.7}NaY$ sample. Before discussing the possible reasons of this different behavior as a function of the desorption temperature, we will consider Fig. 4 on which νCO, derived from Figs. 2 and 3, has been plotted versus the desorption temperature.

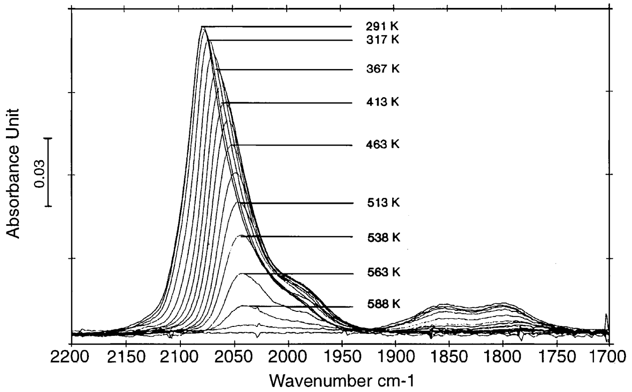

FIG. 2. IR spectra of CO adsorbed on $Pt_{1.7}NaY$ at room temperature and desorbed at different temperatures.

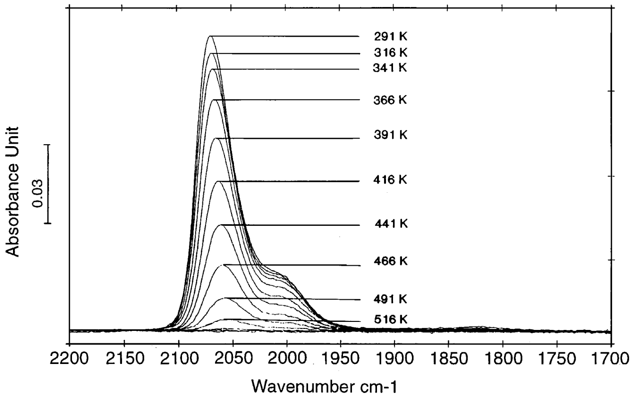

FIG. 3. IR spectra of CO adsorbed on $Pt_{1.7}Sn_{0.9}NaY$ at room temperature and desorbed at increasing temperatures.

This figure shows that on $Pt_{1.7}NaY$ the νCO shifted by only 2 cm^{-1} while the temperature increased from 543 to 573 K and the coverage by CO decreased from less than 0.1 to almost 0.

Hence the different νCO frequencies (2045 cm^{-1} for $Pt_{1.7}$ NaY; 2056 cm^{-1} for $Pt_{1.7}Sn_{0.9}NaY$) measured at 543 K and surface coverage less than 0.1 (almost 0 for $Pt_{1.7}Sn_{0.9}NaY$) cannot be explained either by temperature effect nor by CO coverage effect. At such low CO coverage since the dipolar interaction between two Pt–CO singletons is neglegible, the νCO frequency of the Pt–CO singleton vibrator is sensitive to

— the metal particle size,
— the electronic effect due to a modification of Pt properties resulting from the alloying of Pt with Sn.

The first factor, particle size effect, is probably at the origin of scattered results reported for Pt supported on Al_2O_3 (11) or on SiO_2 (12). In a recent study devoted to the CO adsorption on Pt/SiO_2 (13), it has been shown that depending on the coordination number, the νCO frequency (singleton vibrator) was changing from 2085 cm^{-1} for Pt atoms with a coordination number of 9 to 2057 cm^{-1} for Pt atoms having a coordination number of 6. Similar effects, increase of νCO with the increase of the particle size diameter, were reported for iridium on alumina (14). The second factor, change of the electronic properties of Pt by Sn addition, should induce an opposite effect: it is generally accepted that the electronic effect (if it exists) due to the shift of electron density from Sn to Pt would induce a shift of νCO toward lower wave numbers.

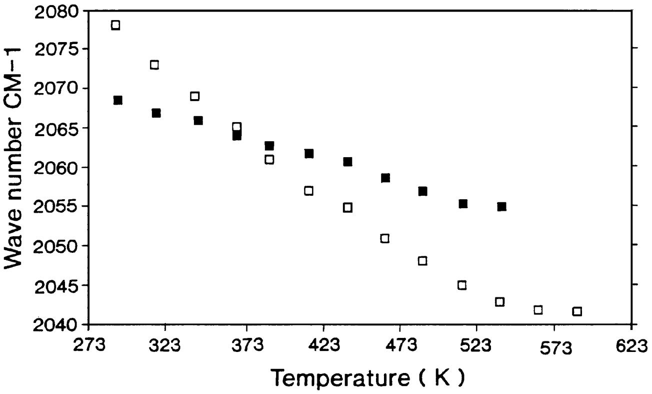

FIG. 4. TPD of CO. Change of CO singleton frequency as a function of the desorption temperature. □, $Pt_{1.7}NaY$; ■, $Pt_{1.7}Sn_{0.9}NaY$.

Indeed, if the two phenomena occur simultaneously, the resulting νCO shift will be the sum of two opposite effects. Here, due to the experimental procedure used (deposition of Sn on preformed Pt particles) a particle growth is expected and indeed observed (7): it has been shown by TEM that the particle sizes are definitly larger for $Pt_{1.7}Sn_{0.9}NaY$ than for $Pt_{1.7}NaY$ (7).

Thus, from IR results, it is concluded that if an electronic effect exists, its importance, relative to the particle size effect, is small. In a recent paper, Passos *et al.* (15) reported that for $PtSn/Al_2O_3$, the major effects of the addition of Sn to Pt, as far as IR of CO is concerned, is a particle size effect and a dilution effect. Similar conclusions were derived from another recent study (16).

The examination of the IR results of Passos *et al.* (15) also indicates that the desorption of CO occurred at a lower temperature for $PtSn/Al_2O_3$, than for Pt/Al_2O_3, in good agreement with our CO TPD data.

It is unlikely that the lower temperature needed to desorb CO from $Pt_{1.7}Sn_{0.9}NaY$ is only due to a particle growth as observed by TEM. More likely this difference should be explained by the preferential blocking of the most reactive platinum atoms by tin. Such hypothesis is consistent with the method which has been used to prepare the tin-based sample (reaction of tetramethyltin with hydrogen chemisorbed on Pt atoms (7)).

CATALYTIC RESULTS

Dehydrogenation of Propane

The reaction was studied in the range of 595 to 693 K. The experimental conditions (WHSV) were fixed such that the conversions were low and not limited by the thermodynamic; in all cases, it has been checked that the rate of propane dehydrogenation was not limited by external diffusion.

In order to avoid serious deactivation, the reaction was run under the following conditions: Reaction was run for 0.5 min and the reactor was flushed with hydrogen for 15 min before running another test. For each sample, temperature was varied up and down 723 K and the last experimental point was run under experimental conditions identical to those utilized for having the first experimental point. The agreement between the experimental values obtained for the first and last experimental point was nearly

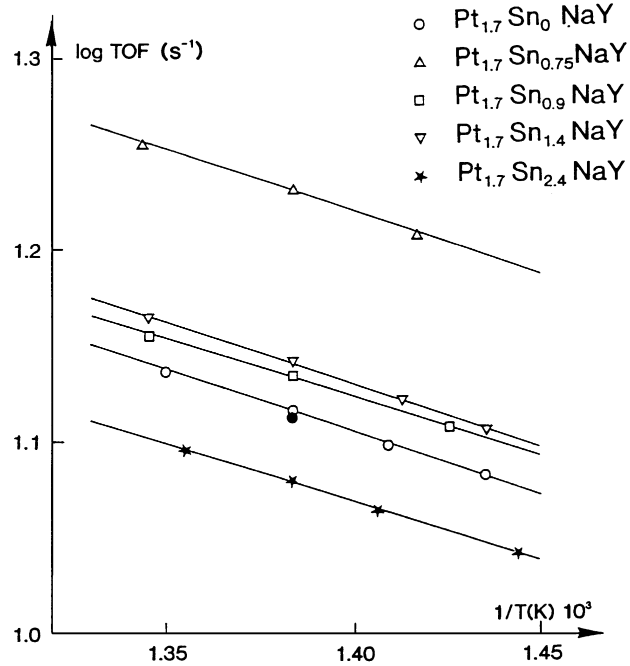

FIG. 5. Dehydrogenation of propane on Pt and PtSn samples. Arrhenius plots. $P_{C_3H_8} = 26.5$ kPa.

perfect except for the PtNaY sample for which a small deactivation was observed (see Fig. 5, last experimental point, ●).

In Table 1 the data relative to $Pt_{1.7}Sn_xNaY$ samples are summarized.

Under the experimental conditions used, dehydrogenation of propane without adding hydrogen, the selectivity to propene (number of molecules of propene formed/number of molecules of propane transformed) is between 0.995 and 1.

The rate of propene formation per gram of solid (see Table 1, column 2) decreased when the tin loading was increased; it has been shown in a previous publication that the Pt dispersion, as measured by H_2 chemisorption, was also decreased by tin addition (7).

Thus the TOF (Table 1, column 3) calculated by using Pt dispersion measured previously (7) is not much modified by the tin addition. The TOF of $Pt_{1.7}NaY$ is probably slightly under estimated: it has been indicated above that for all samples except $Pt_{1.7}NaY$, the experimental conditions used here (bracketing technique) induced no deactivation.

For $Pt_{1.7}NaY$, even with the bracketing technique, a small deactivation is observed (see Fig. 5, last experimental point, ●).

In contrast, for all samples, when using a continuous flow reactor, deactivation is observed, $Pt_{1.7}NaY$ sample deactivating faster (Fig. 6).

The increase in stability, due to tin addition, has already been reported and suggests that coke formation on Pt is also a demanding reaction.

The small changes observed for TOF as a function of tin loading clearly indicated, as reported earlier, that the alkane dehydrogenation reaction proceeds on small ensemble of surface platinum atoms (18). Since the exact composition of the bimetallic PtSnNaY surface is not known (7) it is not possible to determine if the required Pt ensemble is larger than 1 (18). In Fig. 5 the Arrhenius plots obtained for different samples are represented.

TABLE 1

Dehydrogenation of Propane at 723 K

Catalyst	Rate of propene formation mmol h^{-1} g^{-1} catalyst	TOF^a (s^{-1})	$E_a{}^b$ (kJ/mol)
$Pt_{1.7}Sn_0NaY$	3890^c	13^c	62.7
$Sn_{0.75}$	2193	16.9	62.7
$Sn_{0.9}$	1563	13.6	58.5
$Sn_{1.4}$	1100	13.8	62.7
$Sn_{2.4}$	611	12.0	58.5

Note. $P_{C_3H_8} = 26.5$ kPa; P_{total} = atmospheric pressure.

[a] Calculated by using Pt_s/Pt values reported in (7).

[b] Apparent activation energy measured by varying T in the range of 595–653 K (see Fig. 7).

[c] This value is probably underestimated due to the aging of the catalyst (see Fig. 5).

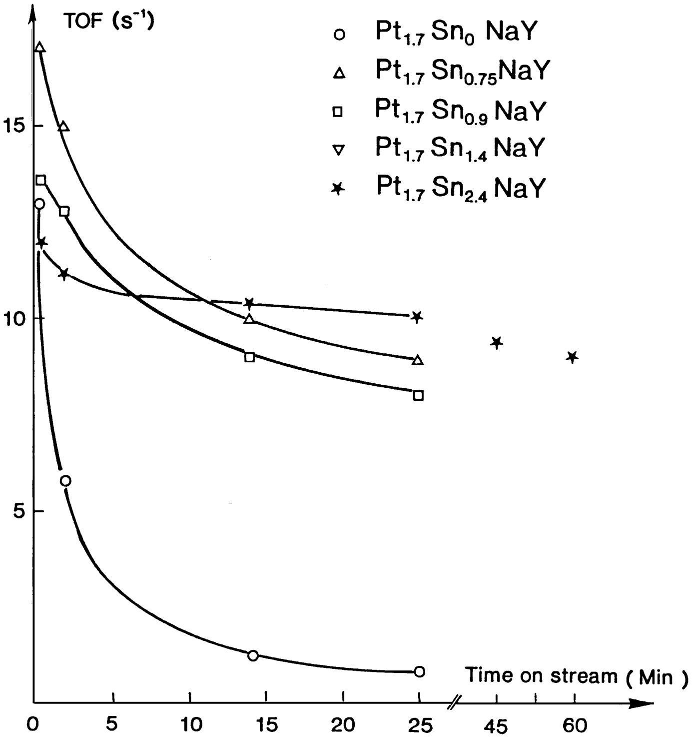

FIG. 6. Dehydrogenation of propane over Pt and PtSnNaY samples. Deactivation versus time on stream.

The same apparent activation energy measured for all catalysts suggests that the rate limiting step is the same regardless of the surface composition.

The value of the apparent activation energy of propene formation is of the same order of magnitude than that measured for D_2/isobutane exchange over Pt and PtSn catalysts (6). This suggests that in the case of propane dehydrogenation the first step of the reaction

$$C_3H_8 + 2\,Pt \rightarrow C_3H_7Pt + Pt{-}H$$

could be the rate limiting step.

Hydrogenolysis of Propane

The hydrogenolysis of propane is a reaction which occurrs simultaneously with the dehydrogenation reaction. Under the experimental conditions used here, relatively high temperature, ratio of propane/hydrogen ~1 and 26.5 kPa of propane, the propene formed is at the equilibrium with propane. As a consequence, propene will not be considered further.

As for the dehydrogenation studies (previous section) the bracketing method used here allows to minimize the deactivation and the results are considered as obtained on clean surface.

Examination of Table 2 indicates that the rate of propane hydrogenolysis is deeply affected by the presence of tin: the higher is the tin content, the lower is the hydrogenolysis activity. $Pt_{1.7}Sn_{1.4}$ and $Pt_{1.7}Sn_{2.4}$ samples are inactive for the hydrogenolysis reaction.

Examination of Fig. 7 indicates that the apparent activation energy is not much changed with the tin addition. For pure PtNaY, the apparent activation energy is 159 kJ, a value slightly lower than that reported for Pt/SiO_2 (19). Adding 0.75 wt% of Sn to PtNaY sample does not change the apparent activation energy of the reaction but in contrast the hydrogenolysis rate is decreased by a factor of 10. Since the kinetic parameters (apparent activation energy, order of reaction relative to H_2 and alkane) (see Figs. 8 and 9) are not significantly modified it is suggested that the main effect of the early first Sn amount is a decrease in the number of Pt ensembles able to catalyze the propane hydrogenolysis rather than a change in Pt electronic properties.

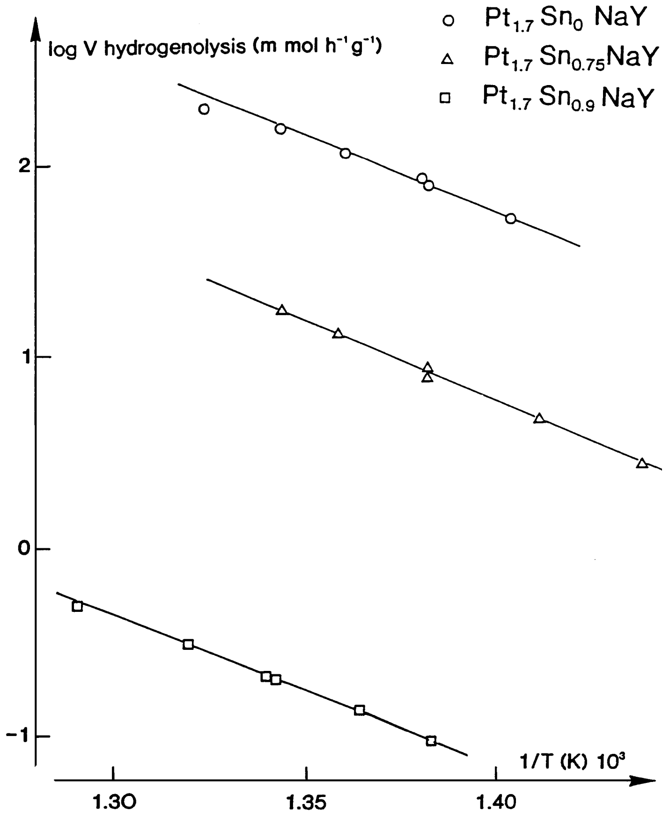

FIG. 7. Propane hydrogenolysis over Pt and PtSnNaY samples. Arrhenius plots obtained with $P_{C_3H_8} = 26.5$ kPa; $P_{H_2} = 26.5$ kPa.

TABLE 2

Hydrogenolysis of Propane over $Pt_{1.7}Sn_xNaY$ Catalysts

Sample	C_3 hydrogenolysis rate^a mmol h^{-1} g^{-1} catalyst	$E_a{}^b$	$O_{HC}{}^c$	$O_{H_2}{}^d$
$Pt_{1.7}Sn_0NaY$	78	159	−0.2	−0.5
$Sn_{0.75}$	7.8	159	0	−0.5
$Sn_{0.9}$	0.1	148	0.3	0
$Sn_{1.4}$	0	—	—	—
$Sn_{2.4}$	0	—	—	—

Note. $T = 723$ K; $P_{HC} = 26.5$ kPa; $P_{H_2} = 26.5$ kPa; P_{total} = atmospheric pressure.

[a] For all samples, $C_3 \rightarrow C_1 + C_2$, with $V_{C_1} = V_{C_2}$.

[b] Apparent activation energy in kJ/mol, as measured in Fig. 7.

[c] Propane apparent order, as measured in Fig. 9.

[d] Hydrogen apparent order, as measured in Fig. 8.

When Sn loading is increased from 0.75 to 0.9 wt%, again the rate of propane hydrogenolysis decreased more, the apparent activation energy only very slightly decreased.

The nearly constant apparent activation energy for all three catalysts suggests that the rate limiting step is the same, independent of the surface composition. This activation energy value, which is much higher than that of the propene formation (previous section) corresponds to the C–C bond breaking.

The change in the hydrogen order (from 0.5 for pure Pt to 0 for $Pt_{1.7}Sn_{0.95}NaY$ sample) and the reverse change in the propane order (from −0.2 to 0.3) with the Sn addition suggest that the the alkane and hydrogen coverages are changing when Pt is alloyed with tin. In a recent study, Cortright and Dumesic (16), studying PtSn bimetallics on SiO_2 (Sn/Pt atomic ratio varying from 0 to 3), have shown that the heat of H_2 adsorption was not modified by adding Sn to Pt (except for high Sn/Pt ratio) (17), but in contrast, for ethylene, the heat of adsorption is reduced of 150 kJ/mol for pure Pt to 115 kJ/mol for PtSn/SiO$_2$ (Sn/Pt = 1.5).

Passos *et al.* (15) have shown for PtSn/Al$_2$O$_3$ that there is no significant change in the hydrogen heat of adsorption compared to Pt/Al$_2$O$_3$. Similar results were reported for PtIn/Al$_2$O$_3$ (15) or for PtInNaY (20). In contrast, for PtIn/NaY the initial heat of adsorption of butane is lower than for PtNaY.

Thus, for propane hydrogenolysis, it can be proposed that compared to Pt, Pt$_{1.7}$Sn$_{0.9}$ surface is saturated with adsorbed hydrogen atoms even for low H$_2$ pressure, this being due to the weakening of Pt–propane bonding. The positive propane order obtained is in agreement with this picture.

Indeed, a change in the propane adsorption constant could be related either to a change of Pt electronic properties or to a change in the Pt ensemble sizes (dilution effects). The results obtained by using CO probe and IR spectroscopy are in favor of the second explanation.

CONCLUSIONS

TDP of CO has shown that the addition of Sn to Pt, forming a bimetallic material, is at the origin of the weakening of Pt–CO bond strength; this weakening of the Pt–CO bond has been attributed to the preferential blocking of higher binding sites by tin rather than a change in the electronic properties of Pt. The IR study of adsorbed CO indicates that at low CO coverages, νCO is lower for PtNaY than for PtSnNaY, this being attributed to a particle growth rather than to a change in electronic properties induced by Sn addition.

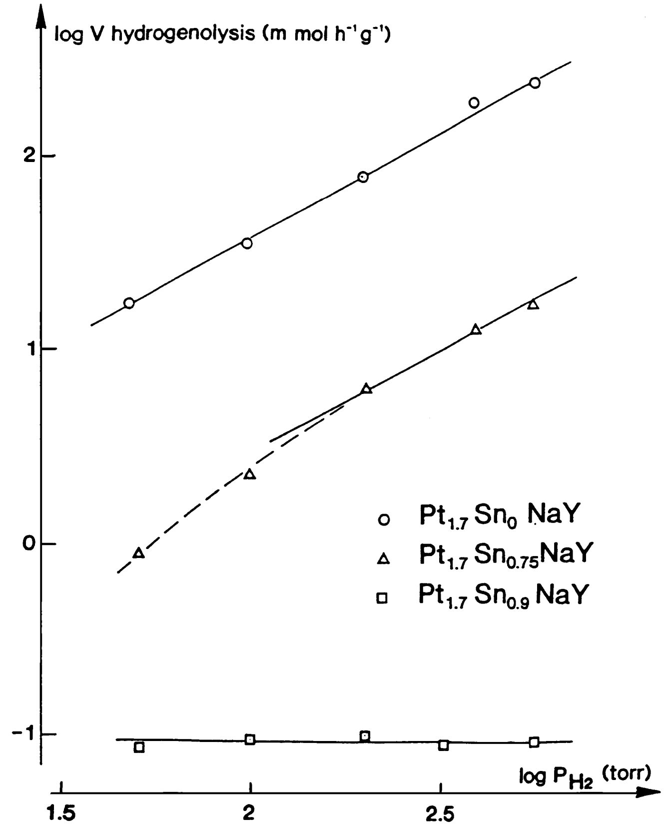

FIG. 8. Propane hydrogenolysis. Log ($V_{\text{hydrogenolysis}}$) = f P(hydrogen) for Pt and PtSnNaY samples. T = 623 K; $P_{C_3H_8}$ = 26.5 kPa.

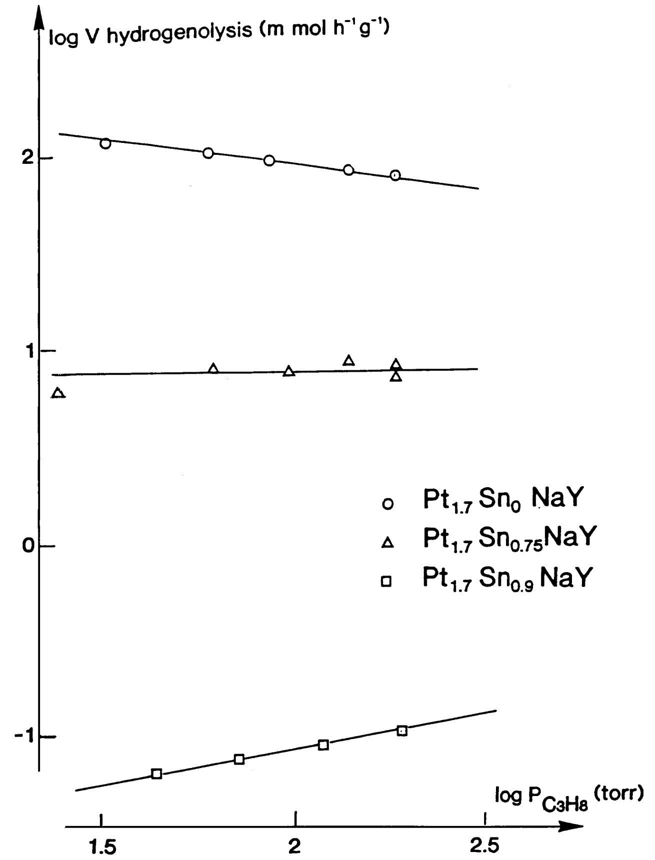

FIG. 9. Propane hydrogenolysis. Log ($V_{\text{hydrogenolysis}}$) = f P(propane) for Pt and PtSnNaY samples. T = 623 K; $P_{C_3H_8}$ = 26.5 kPa.

The catalytic properties, studied by using propane hydrogenolysis and propane dehydrogenation, indicated that the major difference between Pt and PtSn samples are due to a pure geometric effect rather than to an electronic effect.

REFERENCES

1. Sinfelt, J., "Bimetallic Catalysts." Wiley, New York, 1983.
2. Srinivasan, R., and Davis, B. H., *Platinum Met. Rev.* **36**, 151 (1992) and references of Davis, B. H., herein.
3. Lieske, H., Sarkany, A., and Völter, J., *Appl. Catal.* **30**, 69 (1987) and references to other works by these authors herein.
4. Burch, R., *J. Catal.* **71**, 348 (1981).
5. Szanyi, J., Anderson, S., and Paffett, M. T., *J. Catal.* **149**, 438 (1994) and references of Paffett, M. T., herein.

6. Cortright, R. D., and Dumesic, J. A., *Appl. Catal. A* **129**, 101 (1995) and references of Dumesic, J. A., herein.
7. Mériaudeau, P., Naccache, C., Thangaraj, A., Bianchi, C. L., Carli, R., Vishvanathan, V., and Narayanan, S., *J. Catal.* **154**, 345 (1995).
8. Agnelli, M., Louessard, P., El Mansour, A., Candy, J. P., Burnonville, J. P., and Basset, J. M., *Catal. Today* **6**, 63 (1989).
9. Echoufi, N., and Gelin, P., *J. Chem. Soc. Farad. Trans. I* **88**, 1067 (1992).
10. Mériaudeau, P., Thangaraj, A., Gelin, P., and Naccache, C., *J. Catal.*, in press.
11. Barth, R., Pitchai, R., Anderson, R. L., and Verykios, X. E., *J. Catal.* **116**, 61 (1989).
12. Bartok, M., Sarkany, J., and Sitkei, A., *J. Catal.* **72**, 236 (1981).
13. Brandt, R. K., Hughes, M. R., Bourget, L. P., Truszkowska, K., and Greenler, R. G., *Surf. Sci.* **286**, 15 (1993).
14. Toolenaar, F. J. C., Bastein, A. G. T., and Ponec, V., *J. Catal.* **82**, 35 (1983).
15. Passos, F., Schmal, M., and Vannice, M. A., *J. Catal.* **160**, 106 (1996).
16. Balakrishnan, K., and Schwank, J., *J. Catal.* **138**, 491 (1992).
17. Cortright, R. D., and Dumesic, J. A., *J. Catal.* **148**, 771 (1994).
18. Biloen, P., Dautzenberg, F. M., and Sachtler, W. M. H., *J. Catal.* **50**, 77 (1977).
19. Bond, G. C., and Yide, X., *J. Chem. Soc. Faraday Trans. I* **80**, 969 (1984).
20. Mériaudeau, P., Auroux, A., and Viornery, C., submitted for publication.